Morris and Newell, Proc MIUA, 1998, Leeds

Location of the Optic Nerve Head Boundary.

Dr. T. Morris and Mrs Z. Newell.

Department of Computation, UMIST, PO Box 88, Manchester, M60 1QD.

Abstract. Glaucoma is one of the largest causes of preventable blindness, accounting for 13% of the patients registered as blind in the U.K. The disease induces nerve damage in the optic nerve head, the region of the retina where nerve fibres pass through the eyeball, via increased pressure in the ocular fluid. It is detected and the progress of treatment is assessed in a number of ways, one of which is by noting changes to the shape of the nerve head. We have previously reported manually assisted methods of locating the nerve head boundaries and have demonstrated that clinically useful measurements can be derived. In this paper we report our initial work in automatically locating the nerve head boundaries using a multiresolution technique in which the undesired structures in the image are removed by blurring and the initial boundary information indicated by differentiation in eight directions. The image data is then rectified and thresholded. The results derived in the different directions are combined to give an initial estimate of the boundary location which will by improved by shrinking a dynamic contour onto it to yield a continuous and accurate boundary.

1 Purpose

Segmentation is the generic name given to any process whose function is to divide an image into its constituent components. In many texts the subject is treated simplistically and the components are implicitly identified as discrete objects; the segmentation process is therefore reduced to the problem of differentiating between the objects in the image and the background, and possibly separating the objects. In reality the problem is much more complex since the image may be viewed at a multitude of levels: the components could be objects or parts of objects, each existing at a range of sizes. It is the task of the segmentation process to identify the separate objects in the image, their constituent parts and their interrelationships. This paper will describe our initial attempts at deriving such a segmentation process, and its application to segmenting images of the optic nerve head. Traditional image processing techniques are incapable of segmenting these images as required. For example, simple edge detection operators emphasise the vessel boundaries but respond weakly if at all to the required boundaries; model based techniques such as the Hough transform are inappropriate due to the wide variation in the shape of the boundaries.

Whilst most of the principles underpinning our approach to segmentation are generally applicable, it is not possible to apply our detailed implementation to other segmentation problems since many application specific details are encoded. We have observed that this is generally true, even with such low level algorithms as segmentation it is not possible to produce generic solutions.

The optic nerve head images contain two major components: a network of blood vessels and the nerve head itself consisting of an outer rim (separating the nerve head and the retina) and an inner rim. The blood vessels and nerve fibres serving the retina are located on the eye's inner surface. They pass through the eye at the optic nerve head (the "blind spot"). This structure is sensitive to increases in intraocular pressure (IOP) such as are associated with glaucoma: as the IOP increases, nerve cells at the optic nerve head are killed and the patient eventually notices a loss of sight unless the IOP is reduced surgically or by medication [1, 2]. These images provide a suitable vehicle for demonstrating segmentation algorithms: they contain structures at a range of scales, whose boundaries are indistinct and partially obscured. Samples of a normal and a grossly abnormal optic nerve head are shown in figures 1 and 2.

Identifying the vasculature of the nerve head allows image landmarks to be defined. These are useful when making temporal comparisons of the structure. Of more importance in this application is the identification of the nerve head boundaries themselves. The outer boundary remains an approximately circular structure (it appears elliptical due distortions introduced by the imaging process). In normal eyes the inner boundary is also approximately circular, but it becomes elongated in cases of glaucoma. Once the two boundaries have been identified, their relative sizes could contribute to the diagnosis of glaucoma and will contribute to the assessment of its treatment.

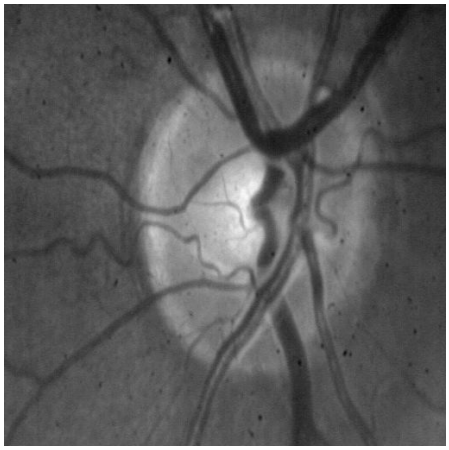

Figure 1
Normal Optic Nerve Head

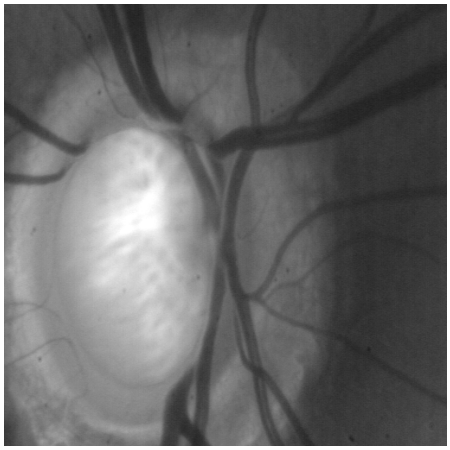

Figure 2
Grossly Abnormal Optic Nerve Head

2 Methods

The methodology of image capture was described in [2], this section will describe the segmentation algorithm. An image was segmented by firstly convolving it with a set of Gabor like kernels [3] and secondly determining those pixels deemed to contribute to the boundary of the object being sought, i.e. initially the optic nerve head outer rim.

The kernels may be thought of as being derived from the "difference of Gaussian" function. They may be computed by differentiating a Gaussian function in one of a number of directions:

$$G(\theta, \mathbf{r}, s) = D_\theta\, g(\mathbf{r}, s)$$

where D_θ represents the directionally dependent differential operator and $g(\mathbf{r}, s)$ the Gaussian function.

Scale information was extracted by using an appropriate sequence of s values. Following [4, 5, 6] the values of s were increased exponentially according to

$$s = \exp(n\,\delta t)$$
$$n = 0, 1, 2, \ldots$$

A value of 0.37 was used for δt, determined by experimentation. The size of the kernel required to represent this function increases slightly faster than $2\pi s$; a kernel of 41 by 41 elements was required for a value of s of 4.4. The first five values of the sequence of s, the values we used, were

$$1.0, 1.4, 2.1, 3.0, 4.4$$

Directional information was derived by differentiating the image in eight equally spaced orientations using a Sobel type operator. In combination, the five scale values and the eight orientation values generated 40 direction dependent feature detectors which were applied to our images. Sample results are presented below of convolving the image of figure 1 with the 135° filters.

Having enhanced the boundaries, we had to identify them in the most blurred images. It was appropriate to use these images as the information retained in them most closely matched the scale of the features we were seeking. If smaller features, such as the vasculature, were being sought, we would use a less smoothed set of

images. Identification was achieved by firstly rectifying the data so as to obtain absolute values of the differentiated data and then secondly thresholding it. The threshold was determined automatically: it was the value that divided the image histogram such that the average of the averages of values less than and values greater than the threshold equalled the threshold. The results were further processed by retaining only the results pertinent to the directional operator's quadrant, the remainder of the image was set to zero.

The results obtained via each of the directional kernels were combined to indicate some of the required boundary information: some information was lost due to poor contrast in the original image or by being obscured by other structures. The major difficulty at this stage of the algorithm is filling in the lost portions of the boundary, a problem solved in previous systems we have developed by inserting a straight line section [7, 8] or by using dynamic contours (snakes) [9].

Once boundary evidence has been gathered from the most blurred image, it is necessary to link it down to the least blurred image since a consequence of the blurring is a loss of spatial accuracy. We use heuristics adapted from [4] for this purpose. This portion of the system is still under development.

3 Results

Figure 3 presents the results of applying the 135° orientation filters to the sample image of figure 1. The pixel data has been offset and scaled to one byte, consequently, a zero response is presented as mid grey, positive and negative responses, indicative of edge information are presented as brighter or darker values. A frame of unconvolved data remains bounding the convolved data in each image where the kernel overlaps the boundary of the image and the convolution is therefore not defined.

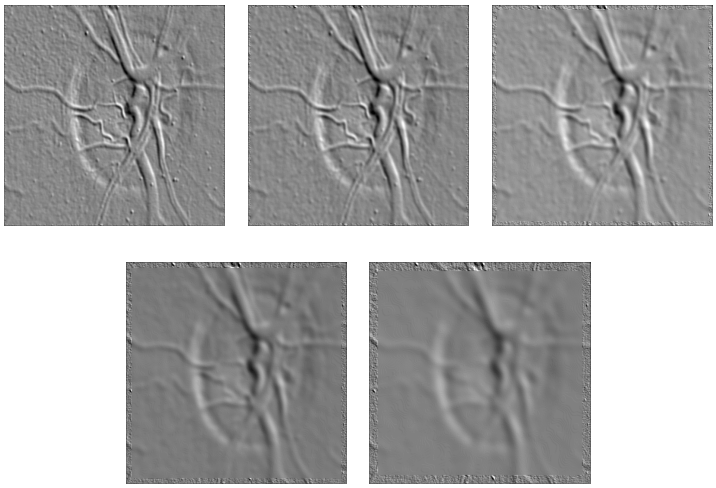

Figure 3.
Results of convolving figure 1 and the 135° filters, s = 1.0, 1.4, 2.1 (top) and 3.0 and 4.4 (bottom).

Figure 4 illustrates the effect of rectification, i.e. taking the absolute result of the convolution process. Brightness values in this image correlate with edge strength irrespective of the sense of the edge. Some blood vessels respond strongly since their size and orientation match those picked out by this kernel. The required nerve head boundary also responds strongly in the bottom left quadrant, as expected. The results obtained by the other kernels at this scale are qualitatively similar.

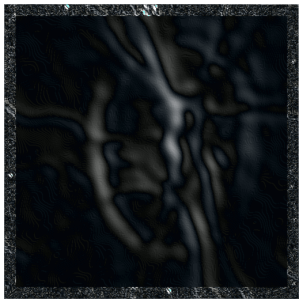

Figure 4.
Rectified version of most smoothed image of figure 3.

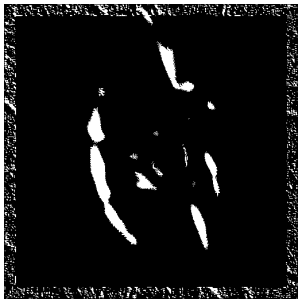

Figure 5.
Thresholded version of figure 4.

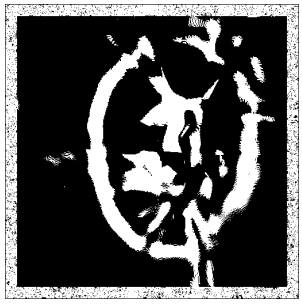

Figure 6.
Enhanced Boundary Pixels.

Figure 5 shows the result of thresholding the data of figure 4. We may ignore the frame of the image (as above) and see that the nerve head and vessel boundaries appropriate to this kernel's size survive. The break in the boundary at the 9 o'clock position is due to a blood vessel. We take the output of all kernels at this scale, set the irrelevant data to zero and combine them logically. A sample of the combined information is shown in figure 6.

4 Summary and Discussion

We aim to produce an algorithm that is capable of delineating the optic nerve head boundaries in a monochrome image of that structure. The nerve head's shape will then be assessed using simple measures that have been shown to be effective in quantifying the changes that are known to occur in glaucoma. This will give optometrists an additional tool in managing this disease.

Thus far, we have developed software to enhance the required boundaries using Gaussian smoothing and differentiation. From this set of enhanced images, we may isolate structures of differing characteristic sizes (scales) such as the vasculature in this region or, in this application, the nerve head boundaries.

Pixels contributing to the nerve head boundaries are suggested in the most smoothed images by taking the magnitude and thresholding. The boundary information from this set of images is combined into a single image, and a dynamic contour (snake) will be shrunk onto it. The snake algorithm has the attractive properties of outlining the boundary where it is found and interpolating where it is missed.

Smoothing the image may displace the boundary pixels from their correct locations. These are regained by tracing these pixels back through the hierarchy of smoothed images. Simple heuristic rules have been suggested for linking pixels between the layers of the hierarchy. This portion of the system is under development.

In addition to this software, we shall investigate additional enhancement of the images prior to this processing. The aim here would be to improve the reliability of our processing by reducing the noise and improving the contrast of the images. The subject and image capture device combine to give poor quality images!

The final portion of this ongoing research is to test the algorithm. For this purpose we have a set of some 500 retinal images derived from normal and glaucoma patients.

Acknowledgements

Mrs Newell is partly funded by the International Glaucoma Association.

References

1. Y. Mo, D. Xiao. “Recognizing the glaucoma from ocular fundus image by image analysis.” (sic) *Proceedings of the 12th Annual International Conference of the IEEE Engineering in Medicine and Biology Society*. Philadelphia, November 1990.
2. M.J. Cox, I.C.J. Wood. “Computer-assisted optic nerve head assessment.” *Ophthal. Physiol. Opt.*. **11,** 1991, 27-35.
3. D. Gabor. “Theory of Communications.” *J. Inst. of Elect. Eng*. **93**, 1946, 429-457.
4. A.S.E. Kostner at al. “Heuristic linking methods in multiscale image segmentation.” *Comp Vision Image Understanding.* **65(3)**, 1997, 383-402.
5. L.M.J. Florack at al. “Cartesian differential invariants in scale space.” *J Math Imaging Vision.* **3**, 1993, 327-348.
6. J.J. Koenderink, “The structure of images.” *Biol Cybernetics.* **50**, 1984, 363-370.
7. D.T. Morris, M.J. Cox, I.C.J. Wood. “Automated Extraction Of The Optic Nerve Head Rim.” *American Association of Optometrists Annual Conference*, Boston, December 1993.
8. T. Morris, I. Wood. “The Automatic Extraction Of The Optic Nerve Head.” *American Academy of Optometrists, biennial European meeting.* Amsterdam, May 1994.
9. T. Morris, C. Donnison. “Identifying the Neuroretinal Rim Boundary Using Dynamic Contours.” *Image and Vision Computing* (in press).